Piezoresistive Elastomer Composites Used for Pressure Sensing

Sara Naderizadeh, Giovanni Santagiuliana, Wei Tu, Derek Marsh, Emiliano Bilotti, and James J. C. Busfield

***Abstract*—Pressure sensors with capability to detect small physical movements and mechanical deformations have been widely used in wearable and medical applications. However, devices that are commercially available currently require complex designs and fabrication and present only a limited force-range sensitivity. To simplify the design, a thermoplastic polyurethane (TPU)/carbon nanotubes (CNTs) composite film has been developed using a melt extrusion technique followed by compression molding. Pressure sensors were made from these films, whose piezoresistive response has been analyzed as a function of the concentrations of CNTs, around the percolation threshold. The changes in the voltage of the device with applied pressure were continuously measured using a voltage divider system coupled with an electromechanical test machine that dynamically loaded the sensors under compression. The voltage divider system was tuned to obtain the best sensitivity and signal/noise (*S*/N) ratio for each device tested. The results showed that sensors containing a target of 2.5 wt% CNTs had market leading sensitivity and repeatability during long-term stability testing and showed high durability during underwater testing, indicating that such devices can be used as a promising robust pressure-sensitive sensor in wearable devices.**

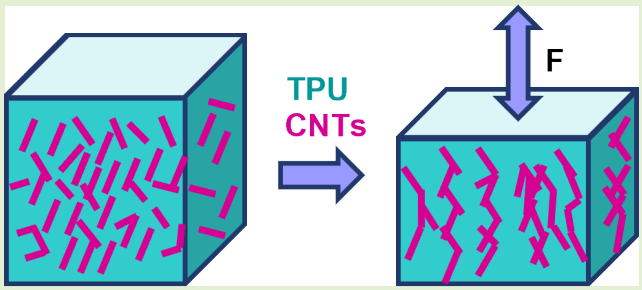

***Index Terms*—Carbon nanotubes (CNTs), electromechanical behavior, piezoresistive, sensor, thermoplastic polyurethane (TPU).**

I. Introduction

FLEXIBLE pressure sensors can be categorized into three main groups, including piezoresistive, capacitive, and piezoelectric, according to their sensing mechanisms [1], [2]. Piezoresistivity, as an important property of conductive materials, enables them to be particularly promising to be used as pressure sensors due to their simple structure and low cost [2]. This property describes the changes in electrical resistance resulting from mechanical deformation of the material [3], [4], [5], [6]. There are many materials, such as inorganic semiconductors and metals that exhibit piezoresistive behavior, which are used in sensor applications. However, due to their inherent rigidity, their applications are limited, especially in wearable devices [7], [8], [9]. Therefore, conductive polymer composites with mechanical flexibility and controllable electrical properties are introduced in the development of such a sensor, by integration of conductive fillers such as carbon nanotubes (CNTs) [10], [11], [12], [13], [14], graphene [15], [16], [17], hybrids of CNTs and graphene [18], carbon black (CB) [14], [19], [20], [21], and metal nanoparticles [22], [23], [24] into a polymer matrix. These discoveries have led to the development of several types of flexible and highly sensitive pressure or strain sensors for different applications, from health monitoring to wearable devices [25], [26], [27], [28], [29], [30], [31], [32], [33], [34]. To achieve suitable flexibility of the sensor, an elastomer with a high elasticity and a low elastic modulus is typically used as a polymer matrix [35], [36]. The most widely selected elastomers in sensor developments are polydimethylsiloxane (PDMS) also known as silicone rubber [37], [38], [39], [40], thermoplastic polyurethane (TPU) [13], [31], [41], [42], and rubber [25], [43], [44].

Manuscript received 13 May 2023; revised 19 June 2023; accepted 19 June 2023. Date of publication 11 July 2023; date of current version 15 August 2023. This work was supported by the Arts and Humanities Research Council, U.K., under Grant AH/S002804/1. The associate editor coordinating the review of this article and approving it for publication was Prof. Kai Wu. *(Corresponding author: Sara Naderizadeh.)*

Sara Naderizadeh and James J. C. Busfield are with the School of Engineering and Materials Science, Queen Mary University of London, E1 4NS London, U.K. (e-mail: s.naderizadeh@qmul.ac.uk; j.busfield@qmul.ac.uk).

Giovanni Santagiuliana was with the School of Engineering and Materials Science, Queen Mary University of London, E1 4NS London, U.K. He is now with Polymateria Ltd., W12 0BZ London, U.K. (e-mail: g.santagiuliana@qmul.ac.uk).

Wei Tu and Derek Marsh are with Nurvv Ltd., TW9 2PR London, U.K. (e-mail: wei@nurvv.com; derek@nurvv.com).

Emiliano Bilotti was with the School of Engineering and Materials Science, Queen Mary University of London, E1 4NS London, U.K. He is now with the Imperial College London, SW7 2AZ London, U.K. (e-mail: e.bilotti@imperial.ac.uk).

This article has supplementary downloadable material available at https://doi.org/10.1109/JSEN.2023.3292239, provided by the authors.

Digital Object Identifier 10.1109/JSEN.2023.3292239

There are already pressure sensors available in the market, which exhibit good performance in many applications [45], [46]. However, their complex design, multilayered structure, often including several printing steps, limited force-range sensitivity, and finally poor environmental stability, restricts their utilization in many potential applications.

In this work, a pressure sensor with a simple structure was fabricated based on TPU as a flexible matrix and using CNTs as the conductive network. The conductive composite films were produced through the melt extrusion technique using a twin screw compounder, followed by hot pressing into a piezoresistive film layer from which the sensors were cut. The electrical properties of the constructed sensors were analyzed using a voltage divider system, which adopts an in-house developed LabVIEW program. A specified load protocol that cyclically loaded the sensor in compression was applied using an Instron ElectroPuls universal test machine, and the force sensitivity, repeatability, long-term stability, and durability of the sensors were all characterized both in air and when exposed to water. Then, these newly developed sensors were compared to a leading commercial sensor to evaluate their sensing performance, load range sensitivity, and long-term durability. The results highlight that the volume fraction of the CNTs in the composite and the selection of suitable reference resistors in the voltage divider system were both essential elements when optimizing the piezoresistivity response.

The simple and scalable fabrication techniques that were used to develop a durable sensor with high sensitivity at different force ranges and excellent repeatability could bring a great potential for these sensors to be used in wearable sensing devices.

II. Materials and Methods

A. Materials

TPU, Estane[1] 58437, an aromatic polyester-based TPU with shore A hardness of 85 ± 3 and density of 1.19 g/cm^3, was purchased from Lubrizol. Multiwalled CNTs, NC7000[2], with an average length of 1.5 μm and an average diameter of 9.5 nm were purchased from Nanocyl S.A.

B. Polymer Compounding

The samples in this work were prepared from a masterbatch of TPU containing a nominal CNTs concentration of 5 wt%. The masterbatch was prepared using a Collin ZK25 twin-screw compounder with a screw length-to-diameter ratio of 42, a screw speed of 200 r/min and a temperature profile from zone 1 to zone 8 (die) of 190/240/200/200/200/200/200/180 °C. The main feeder of the ZK25 compounder was used to supply TPU at a speed of 1.9 kg/h. The TPU pellets were predried at 80 °C overnight before compounding. The side feeding system was used to supply the as-received CNTs into zone 3 of the compounder at a speed of 0.1 kg/h. The extrudate was cooled down in a water bath and pelletized.

The pellets of the masterbatch were then dried at 80 °C overnight before being blended to reduce the CNTs volume fraction with predried, neat TPU and obtain final sample materials with nominal CNTs concentrations of 2.1%, 2.3%, and 2.5%. The blending was done using an Xplore MC15HT micro-compounder operating in the recirculation mode for 3 min in an argon atmosphere with a screw speed of 200 r/min and a temperature of 200 °C. The extrudates were cooled down in ambient air and pelletized.

[1]Registered trademark.
[2]Trademarked.

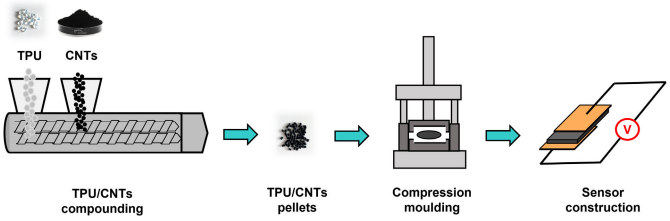

Fig. 1. Schematic of all the steps adopted through sensor construction.

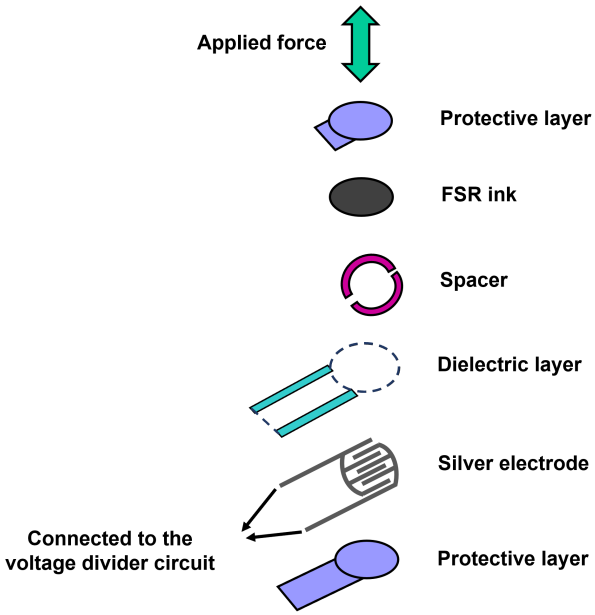

Fig. 2. Schematic of a commercially available sensor.

C. Film Preparation and Sensor Construction

TPU/CNTs blend films with different CNTs proportions were prepared using a hot press machine (Collin E300). The temperature was raised to 185 °C and the compounds were kept at this temperature for 3 min without pressure; then, 100-bar pressure was applied for 30 s, followed by cooling under the same pressure. An aluminum mold of size 300 × 300 mm was used to produce films of size 100 × 100 mm. To construct the sensors, films were cut from the center into 20 × 20 mm pieces with an average of 200 μm thickness and connected to the external wire electrodes using silver paint. The schematic of different steps in sensor fabrication is shown in Fig. 1.

D. Commercial Sensor Structure

An example of a simplified commercial pressure sensor structure is shown in Fig. 2. A force-sensitive resistor (FSR) ink is printed through screen printing technique from a liquid

and cured to make a solid layer. An adhesive spacer is inserted between the FSR ink and a layer of interdigitated electrodes. The small free volume provided by the spacer allows for air to be vented in and out and reaches a pressure equilibrium with the external atmosphere. In this way, the sensor promotes a fast and complete recovery to its initial unloaded state, after each loading cycle through air ventilation. The spacer can also allow for a higher sensitivity at low forces due to the increasing electrical contact between the FSR ink and the interdigitated electrodes as a function of the applied force. A dielectric layer is printed on top of the silver electrode to avoid interference and protect against corrosion. Finally, two outer protective layers, typically made of polyethylene terephthalate (PET), are added to insulate the sensor from the environment. Due to this complex structure that involves several printing steps, which produces a limited force-range sensitivity, the use of these FSR sensors is restricted to a few limited applications. For example, if we consider the case of monitoring human walking and running activities, wearable FSR sensors are required to sense a force within the range of 0–100 N. However, existing commercial sensors do not perform well over this force range and are affected by corrosion at the interdigitated ends and are subject to wearing by the relative sliding between the FSR ink and electrode layers due to the free volume produced by the spacer.

E. Characterization Methods: Thermogravimetric Analysis (TGA) and Scanning Electron Microscopy (SEM)

TGA was used to confirm the CNTs concentrations in the polymer matrix using the TA/TGA5500 instrument. The TPU/CNTs blend pellets were heated up from room temperature to 600 °C at a heating rate of 20 °C/min under an inert nitrogen atmosphere. The tests were repeated three times for each sample. The actual filler content was estimated from the residual weight percentage at 600 °C, and the results are shown in the Supporting Information (see Fig. S1).

SEM was utilized to examine the CNT's dispersion in the TPU matrix. SEM images from cross section were obtained using field-emission scanning electron microscope (FEI Inspect F), OXFORD INSTRUMENTS, with 20-kV acceleration voltage. For cross section SEM imaging, the polymeric films were cryogenically fractured in liquid nitrogen. Before imaging, the samples were sputter-coated with about a 3-nm gold layer on the fracture surface, to reduce charging effects. To prepare the CNTs sample for imaging, a low concentration of about 10 mg/mL CNTs was dispersed in ethanol, sonicated for 3 min, and deposited on a glass slide. After evaporation of ethanol, CNTs were transferred onto a carbon tape and SEM imaging was performed under the same conditions as above.

F. Data Acquisition System

A fundamental circuit widely adopted in electronics is a voltage divider, which produces an output response based on a proportion of its input voltage [5], [47]. In this system,

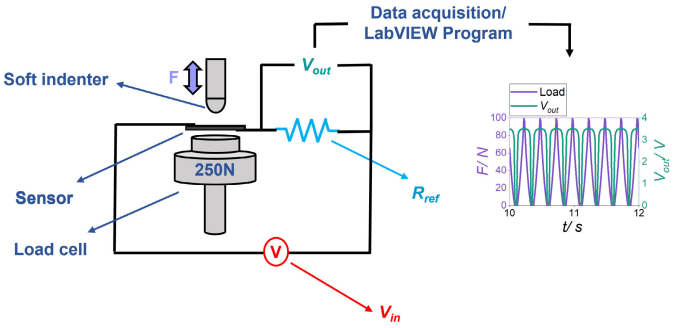

Fig. 3. Schematic of the sensing measurement setup and data acquisition.

a simple and constant known resistor R_{ref} and the sensor are connected in series, as shown in Fig. 3, and attached to a power supply (Rapid dc POWER SUPPLY HY3005D) with a certain input voltage V_{in} (3.5 V was used throughout this work). As the voltage is distributed between the two resistors, one with a known reference resistance and the sensor with an unknown resistance, the output response V_{out} would be a function of the input voltage. As the electrical resistance R_{sensor} of the piezoresistive material changes as a function of the applied force F, the measured output voltage V_{out} of the voltage divider system is also a function of F

$$V_{\text{out}}(F) = \frac{V_{\text{in}} \cdot R_{\text{ref}}}{R_{\text{sensor}}(F) + R_{\text{ref}}}. \tag{1}$$

In this work, an Instron ElectroPuls E1000 machine was used to apply different loading profiles on the sensors while monitoring V_{out} of a voltage divider system using a NATIONAL INSTRUMENTS USB (NI USB-6009) together with the LabVIEW program. A 250-N load cell and a half sphere-shaped soft test indenter made of rubber with 15 mm diameter attached to the actuator were used.

III. Results

A. TPU/CNTs Compound Characterization

Fig. 4(a) shows the percolation threshold trend for CNTs inside the TPU matrix. We estimated the electrical percolation threshold by fitting the conductance values of a series of TPU + x% CNTs composite materials when a very small compressive force of 0.00063 N was applied to ensure a good contact between the materials and the electrode. We could not measure any conductance for materials containing less than 1.5 wt% CNTs. Since the samples had the same thickness and the electrode was the same for every sensor, we did not convert the conductance values into conductivities. We fit the conductance (G) of the sensors with the following conductivity model: $G = G_0(w - w_c)n$, where G_0 is the conductivity of the composite material when the CNTs concentration approaches 100%, w is the CNTs weight concentration, w_c is the percolation threshold, and n is the percolation exponent. We found that the percolation threshold was close to 2 wt% and the sensors with CNTs loading close to the electrical percolation threshold were investigated in this work. In this way, any small compressive force would have a dramatic impact on the

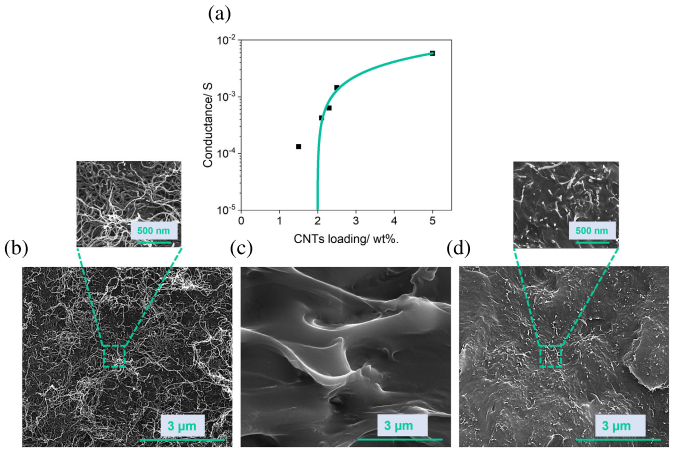

Fig. 4. (a) Illustration of percolation threshold of CNTs inside the polymer matrix. (b) SEM image of the CNTs dispersed in ethanol, and freeze-fractured cross-sectional SEM image of (c) pure TPU and (d) typical TPU/CNTs compound.

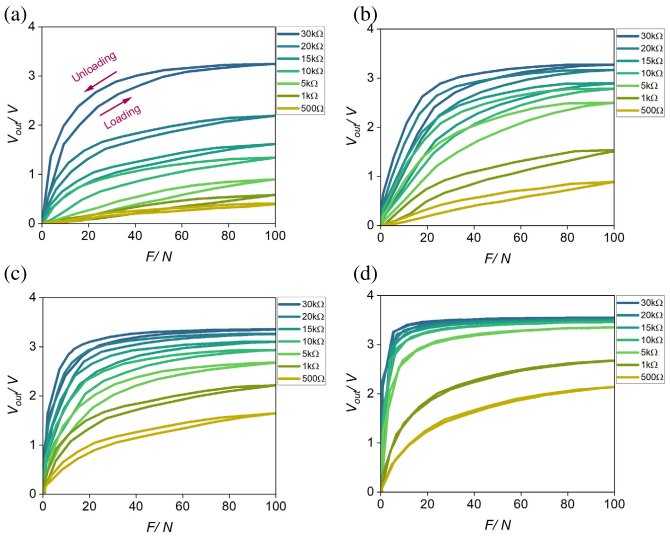

Fig. 5. Output voltage, V_{out} for (a) TPU/2.1% CNTs, (b) TPU/2.3% CNTs, (c) TPU/2.5% CNTs test materials, and (d) commercial sensor with 500-, 1-, 5-, 10-, 15-, 20-, and 30-kΩ reference resistors used in the voltage divider system.

number of conductive paths, which should allow for very high sensitivities.

SEM imaging was used to investigate the distribution of CNTs in the polymer matrix on a cryogenically fractured cross-sectional surface and the results are shown in Fig. 4(d). To have a better understanding of the morphologies, the SEM image of the pure CNTs dispersed in ethanol is shown in Fig. 4(b) and a freeze-fractured unfilled TPU film is shown in Fig. 4(c). In general, strong van der Waals interactions among nanofillers, large surface area, and small dimensions are the main parameters that cause the nanoparticles' aggregations [48]. The results showed that CNTs are relatively well distributed inside the polymer matrix for all the samples, due to the energetic mixing during melt extrusion, which allowed CNTs to become well dispersed inside the molten TPU matrix.

B. Output Response Dependence Upon the Reference Resistor

It is a requirement to have the highest signal intensity over a specified force range of $0 < F < F_{MAX}$. Therefore, a suitable reference resistor with $R_{ref} > R_{sensor}$ (F_{MAX}) should be chosen so that $V_{out}(F_{MAX})$ approaches the applied voltage V_{in} [see (1)] when the maximum force is applied. On the other hand, V_{out} is required to increase as linearly as possible with F to produce increased sensitivity, which is possible only when $R_{sensor}(F) > R_{ref}$. These two opposite requirements imply the need to find a good compromise in the value of R_{ref} used so that V_{out} can approach V_{in} at F_{MAX}without reaching a plateau at lower forces. To investigate the best reference resistor for our sensors when subjected to a compressive force range of 0–100 N, 50 loading and unloading cycles were performed at 4 Hz using a wide range of R_{ref} values from 500 Ω to 30 kΩ. Fig. 5 shows the relation between the applied force range and the sensor output response. For simplicity, only one loading–unloading cycle is shown in Fig. 5 for each reference resistor. (The output response over 50 cycles is shown in the Supporting Information, shown in Fig. S2.)

As expected, the intensity of the output response of each sensor is increased when using higher R_{ref} values. However, V_{out} could reach a plateau well before the maximum force was applied if R_{ref} was too high. Instead, when R_{ref} was small, V_{out} appeared to increase more linearly with the force but could reach only small values within the applied force range. From a qualitative analysis of Fig. 5, the best R_{ref} values for TPU/2.1% CNTs, TPU/2.3% CNTs, and TPU/2.5% CNTs sensors appear to be 20, 15, and 10 kΩ, respectively. The best R_{ref} for the commercial sensor appears to be 1 kΩ.

C. Sensing Performance During a Cyclic Pressure Loading Analysis

To evaluate the potential of the fabricated compounds to be used as a piezoresistive pressure sensor, the sensors were subjected to cyclic pressure loading and unloading tests. All measurements were done for 200 cycles at a frequency of 4 Hz and a constant maximum load of 100 N using the optimized R_{ref} for each sensor. Fig. 6 shows the applied load protocol together with the output response in the form of voltage change from the reference resistor in the voltage divider circuit obtained using the in-house developed LabVIEW code.

The output response V_{out} increased with the applied pressure due to the change in the CNTs percolation network of the piezoresistive composites that became better interconnected with more conductive paths [4]. Moreover, as expected from (1), V_{out} could reach higher values when the sensors contained higher CNTs loadings because the corresponding sensor resistances decreased.

In addition, the enlarged images indicate very stable responses in the maximum recorded voltages throughout the tests. This reflects the repeatability in the output response of the sensors under cyclic loading.

An important observation is the size of the hysteresis loop in each loading–unloading cycle, where the smallest hysteresis is

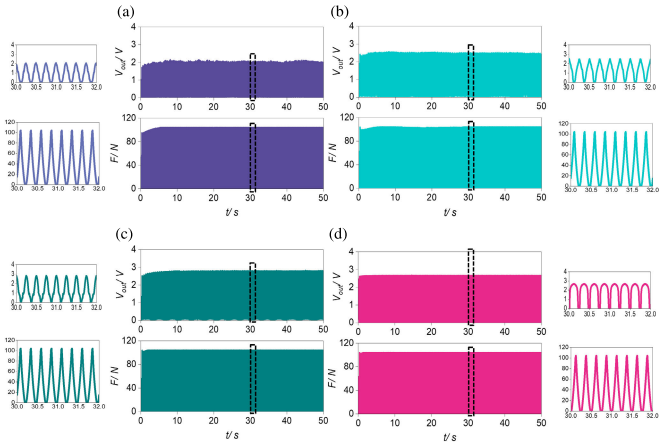

Fig. 6. Applied load and output response for (a) TPU/2.1% CNTs, (b) TPU/2.3% CNTs, (c) TPU/2.5% CNTs, and (d) commercial sensor during cyclic pressure loading/unloading testing. (The zoomed-in region is for 2 s to help visualize the shape of the curves.)

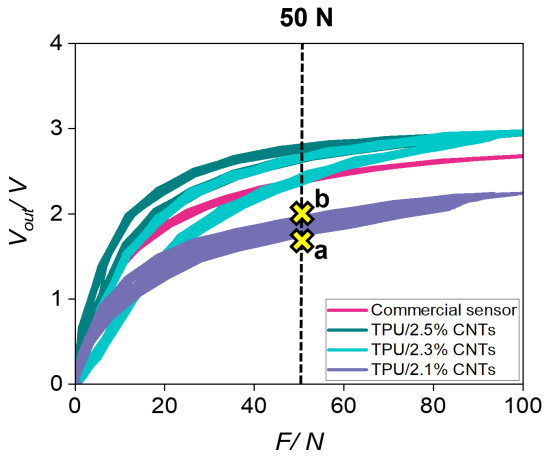

Fig. 7. Output response of 50 loading and unloading cycles on TPU/2.1% CNTs, TPU/2.3% CNTs, and TPU/2.5% CNTs devices and the commercial sensor. (To calculate the hysteresis error, two points with letters a and b at loading and unloading cycles are selected at the midpoint of the graph.)

desirable [2]. This is because a specific output voltage would represent a narrower range of applied force. The electrical hysteresis reflects the normal mechanical hysteresis behavior of the polymer and the filler–polymer interactions [30], [48], [49], [50], [51], [52]. Stronger interfacial interactions between CNTs and elastic polymer networks would possibly produce lower mechanical hysteresis and perhaps increased reversibility in the sensors [53], [54], [55], [56]. In addition, the relaxation behavior of the polymer matrix could also produce a different loading and unloading response, which will contribute to the mechanical hysteresis loop [4].

To examine more closely the hysteresis and recoverability of the sensors, Fig. 7 shows the output voltage of 50 compression loading and unloading cycles when the sensors were connected to their optimum reference resistors as mentioned previously. The hysteresis error of each individual sensor at the midpoint of the graph (at 50 N) was calculated by using (2), where a and b are the output voltage in loading and unloading

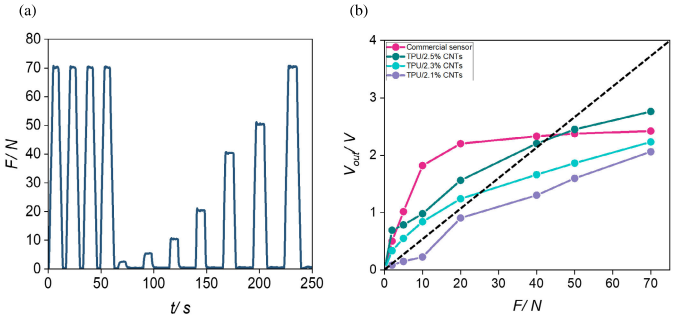

Fig. 8. (a) Load protocol diagram applied using electromechanical test machine. (b) Output response for the TPU/2.1% CNTs, TPU/2.3% CNTs, TPU/2.5% CNTs, and the commercial sensor.

cycles, respectively

$$\text{Hysteresis error}\,(\%) = \frac{(b-a)}{a} \times 100. \tag{2}$$

The commercial sensor shows a small hysteresis of about 1.88% and has good stability after each loading–unloading cycle. Our fabricated sensors, TPU/2.1% CNTs, TPU/2.3% CNTs, and TPU/2.5% CNTs, instead, have higher hysteresis of 6.22%, 9.26%, and 4.47%, respectively. These sensors also show a signal that is less reproducible after each loading–unloading cycle.

D. Sensing Measurement: Force Sensitivity Characterization

To understand the force range sensitivity and the best signal-to-noise (S/N) ratio of the sensors, a loading protocol was developed in which the load was increased from 2 to 70 N gradually [see Fig. 8(a)]. First, all the sensors were subjected to a conditioning cycle, according to which a 70-N load was applied four times with 15-N/s rate and kept for 5 s on the sensors, followed by a 3-s relaxation time in between. Afterward, each sensor was tested under the compressive loadings of 2, 5, 10, 20, 40, 50, and 70 N, which were applied for 8 s prior to being released for 17 s. Fig. 8(b) shows the output voltage of the different sensors when connected to their corresponding best reference resistors as determined previously to have their output signals maximized and their sensitivity optimized. For simplicity, the responses of the sensors during the conditioning cycle are not shown in Fig. 8(b).

The sensors show different sensitivities over different force ranges. For example, TPU/2.1% CNTs sensor does not show any significant sensitivity for small loads below 10 N, and in contrast, the commercial sensor shows a poor sensitivity for higher loads, between 20 and 70 N. Overall, the output response for TPU/2.3% CNTs and TPU/2.5% CNTs sensors cover a wider force range (between 5 and 70 N) and show better sensitivity at each load value.

E. Long-Term Stability Testing

Long-term stability tests were performed up to 50 000 cycles, to assess the performance of the sensors in scenarios relevant to applications as wearable devices and in particular the insoles of smart shoes. A test protocol that

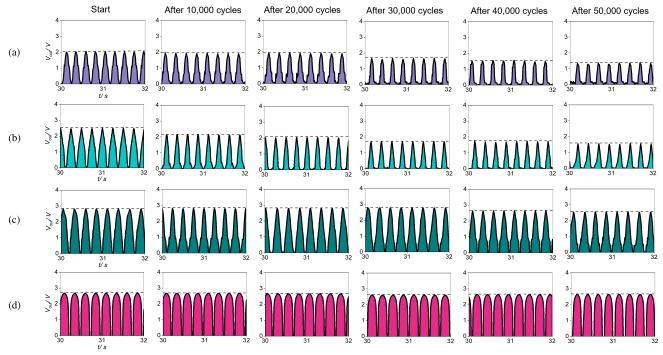

Fig. 9. Long-term stability test results, V_{out} per time for (a) TPU/2.1% CNTs, (b) TPU/2.3% CNTs, (c) TPU/2.5% CNTs, and (d) commercial sensor.

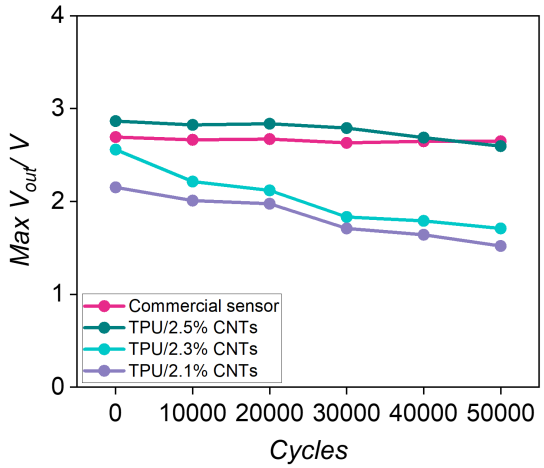

Fig. 10. Output voltage variation over time in long-term stability test.

would simulate a series of five consecutive walking-and-running sequences was chosen (see Fig. 9). In the walking phase of each sequence, a 40-N maximum load was applied at a 2-Hz frequency over 10 000 cycles (about 1 h and 20 min). In the running phase, a 100-N maximum load was applied at a 4-Hz frequency over 200 cycles (50 s). The reproducibility of the voltage output during the five running phases is used as a benchmark to assess the quality of the sensors. As a reference, we performed a preliminary running phase before the long-term tests. Fig. 8 shows the output voltage from our sensors and the commercial device during the preliminary and the subsequent five running phases (to have a better view of the voltage profiles, only eight cycles are shown here).

Fig. 10 shows the stability of the maximum output voltage (Max V_{out}) during the running phases of the long-term tests. Ideally, Max V_{out} should remain constant over time to allow for a reliable conversion of the signal into force. This happens with the commercial sensor as well as our sensor containing 2.5% CNTs. In fact, Max V_{out} of these two sensors decreased only about 2% and 6% over time. The other two sensors containing 2.1% and 2.3% CNTs show lower stability as Max V_{out} decreased by about 35% and 39%, respectively. The viscoelastic behavior of TPU could be the main reason for the decreasing output response during this stability test. This effect is related to the relaxation state of the polymer

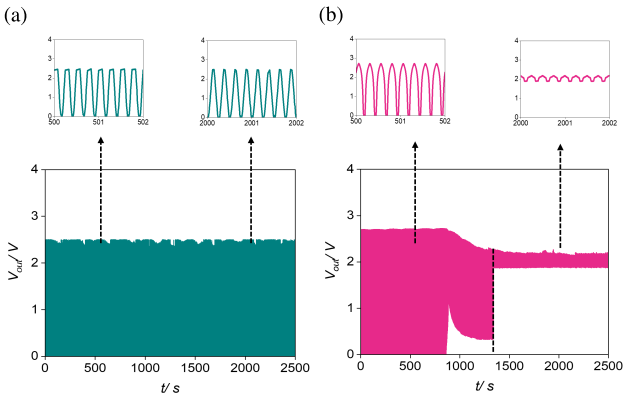

Fig. 11. Durability test results under water ingression (a) TPU/2.5% CNTs and (b) commercial sensor.

matrix, which means that the polymer matrix does not fully recover its initial state [4], which might be improved by crosslinking the TPU. Better filler–polymer interactions might be another parameter that would introduce a more stable response in TPU/2.5% CNTs sensor. Certainly, the improved performance of the TPU/2.5% CNTs over the TPU/2.1% CNTs and TPU/2.3% CNTs comes from the higher CNTs loading and a resulting better interconnected conductive filler network. The application of repetitive forces over time may break down the CNTs network inside the polymer matrix, which corresponds to increase R_{sensor}, hence decreased Max V_{out}. The smaller the CNTs concentration, the more likely the conductive network deteriorates and the higher R_{sensor} becomes. At the end, the commercial sensor shows a stable response without any significant change over time, which is a result of the much more complex sensor design.

F. Durability Testing Under Water Ingress

To further evaluate the suitability for wearable applications, the behavior of the sensors in a wet environment where water could be entered into the sensing area over time was investigated. In this section, only the TPU/2.5% CNTs sensor was compared with the commercial sensor, as it appeared to be the most promising of the sensors tested so far. A protocol of 10 000 loading–unloading cycles at 4 Hz with 100-N maximum force was performed with the sensors being continuously wet by water, which was supplied via a two-channel Ismatec pump at a flow rate of 1.8 mL/min (the schematic of the testing setup is shown in the Supporting Information, Fig. S4). In service, the commercial sensor has an air inlet which we simulated by creating a very small hole with a needle near the sensing area, to allow air and water to pass in over time. The results of this experiment are shown in Fig. 11(a) and (b). The TPU/2.5% CNTs sensor has a much better durability in wet environments compared to the commercial sensor. The baseline of the commercial sensor gradually approaches 1.8 V after about 5000 cycles, and the sensor loses all its force sensitivity. This probably results from water entering the small free volume present inside the structure as discussed in the introduction and affecting the electrodes, which represents a challenge for these types of applications, where the commercial sensor is exposed to outdoor environments. In contrast,

our TPU/2.5% CNTs sensor, which was fabricated with a much simpler and cheaper design without any free volume, did not suffer from this problem. Despite displaying some modest variations in the output voltage, the sensing response was much more stable compared to the commercial sensor.

IV. Conclusion

In this study, a pressure sensor was fabricated by compounding CNTs into a TPU matrix via melt extrusion. A voltage divider system coupled with an ElectroPuls machine was used to apply a compressive load on the sensor and the output voltage of a reference resistor was monitored continuously using an in-house designed LabVIEW program. The effect of various CNTs loadings and the use of different reference resistors in the voltage divider system were studied to optimize the design for maximum force sensitivity and the lowest S/N ratio. To provide a comparison, our fabricated sensors were compared with a commercial sensor in terms of force-range sensitivity, long-term stability, and environmental stability underwater immersion.

The results showed that fabricated sensors have a better sensitivity over a wider force range (5–70 N) compared to the commercial sensor, which showed poor sensitivity at higher loads (20–70 N). On the other hand, the commercial sensor showed a smaller hysteresis loop of 1.88% during loading–unloading cycles, which reflects its better sensitivity compared to the fabricated sensors, TPU/2.1% CNTs, TPU/2.3% CNTs, and TPU/2.5% CNTs, which showed 6.22%, 9.26%, and 4.47%, respectively. However, the TPU/2.5% CNTs sensor showed much better durability when subjected to a water immersion test compared to the commercial sensor. It is worth noting that the TPU/2.5% CNTs sensor displays a better stability during long-term test with respect to the other fabricated sensors, indicating that such device can be used as a promising pressure sensor in wearable devices. However, the functionality can be further improved for practical applications, potentially through crosslinking, to decrease the negative impact of viscoelastic behavior of the polymer, which can influence the hysteresis of the sensor.

Acknowledgment

The authors are grateful for support from Dr. Erica Di Federico and Jun Ma for their assistance with sensing measurement setup. They acknowledge the insightful conversations with Prof. Jane Harris (London College of Fashion, University of the Arts London, London, U.K.).

References

[1] Y. Zang, F. Zhang, C.-A. Di, and D. Zhu, "Advances of flexible pressure sensors toward artificial intelligence and health care applications," *Mater. Horizons*, vol. 2, no. 2, pp. 140–156, 2015, doi: 10.1039/C4MH00147H.

[2] J. Oh et al., "Highly uniform and low hysteresis piezoresistive pressure sensors based on chemical grafting of polypyrrole on elastomer template with uniform pore size," *Small*, vol. 15, Jun. 2019, Art. no. 1901744, doi: 10.1002/smll.201901744.

[3] Y. Zhuang et al., "Preparation and laser sintering of a thermoplastic polyurethane carbon nanotube composite-based pressure sensor," *RSC Adv.*, vol. 10, no. 40, pp. 23644–23652, Jun. 2020, doi: 10.1039/D0RA04479B.

[4] R. Ramalingame et al., "Flexible piezoresistive sensor matrix based on a carbon nanotube PDMS composite for dynamic pressure distribution measurement," *J. Sensors Sensor Syst.*, vol. 8, no. 1, pp. 1–7, Jan. 2019, doi: 10.5194/jsss-8-1-2019.

[5] R. Kõiva, M. Zenker, C. Schürmann, R. Haschke, and H. J. Ritter, "A highly sensitive 3D-shaped tactile sensor," in *Proc. IEEE/ASME Int. Conf. Adv. Intell. Mechatronics*, Jul. 2013, pp. 1084–1089, doi: 10.1109/AIM.2013.6584238.

[6] C. H. Hu, C. H. Liu, L. Z. Chen, Y. C. Peng, and S. S. Fan, "Resistance-pressure sensitivity and a mechanism study of multiwall carbon nanotube networks/poly(dimethylsiloxane) composites," *Appl. Phys. Lett.*, vol. 93, no. 3, Jul. 2008, Art. no. 33108, doi: 10.1063/1.2961028.

[7] P. Ciselli, L. Lu, J. J. C. Busfield, and T. Peijs, "Piezoresistive polymer composites based on EPDM and MWNTs for strain sensing applications," *e-Polymers*, vol. 10, no. 1, p. 14, Dec. 2010, doi: 10.1515/epoly.2010.10.1.125.

[8] J. Teixeira, L. Horta-Romarís, M.-J. Abad, P. Costa, and S. Lanceros-Méndez, "Piezoresistive response of extruded polyaniline/(styrene-butadiene-styrene) polymer blends for force and deformation sensors," *Mater. Des.*, vol. 141, pp. 1–8, Mar. 2018, doi: 10.1016/j.matdes.2017.12.011.

[9] J. R. Dios, C. Garcia-Astrain, S. Gonçalves, P. Costa, and S. Lanceros-Méndez, "Piezoresistive performance of polymer-based materials as a function of the matrix and nanofiller content to walking detection application," *Compos. Sci. Technol.*, vol. 181, Sep. 2019, Art. no. 107678, doi: 10.1016/j.compscitech.2019.107678.

[10] K. N. Dhakal et al., "Electrically conductive and piezoresistive polymer nanocomposites using multiwalled carbon nanotubes in a flexible copolyester: Spectroscopic, morphological, mechanical and electrical properties," *Nano-Struct. Nano-Objects*, vol. 29, Feb. 2022, Art. no. 100806, doi: 10.1016/j.nanoso.2021.100806.

[11] L. Wang et al., "Highly stretchable, anti-corrosive and wearable strain sensors based on the PDMS/CNTs decorated elastomer nanofiber composite," *Chem. Eng. J.*, vol. 362, pp. 89–98, Apr. 2019, doi: 10.1016/j.cej.2019.01.014.

[12] Y. Cai et al., "Stretchable $Ti_3C_2T_x$ MXene/carbon nanotube composite based strain sensor with ultrahigh sensitivity and tunable sensing range," *ACS Nano*, vol. 12, no. 1, pp. 56–62, Jan. 2018, doi: 10.1021/acsnano.7b06251.

[13] Y. Zhou et al., "Significant stretchability enhancement of a crack-based strain sensor combined with high sensitivity and superior durability for motion monitoring," *ACS Appl. Mater. Interfaces*, vol. 11, no. 7, pp. 7405–7414, Feb. 2019, doi: 10.1021/acsami.8b20768.

[14] T. Yamada et al., "A stretchable carbon nanotube strain sensor for human-motion detection," *Nature Nanotechnol.*, vol. 6, pp. 296–301, Mar. 2011, doi: 10.1038/nnano.2011.36.

[15] J. Gao et al., "Electrically conductive and fluorine free superhydrophobic strain sensors based on SiO_2/graphene-decorated electrospun nanofibers for human motion monitoring," *Chem. Eng. J.*, vol. 373, pp. 298–306, Oct. 2019, doi: 10.1016/j.cej.2019.05.045.

[16] J. Kim, E. Lee, G. Mehta, and W. Choi, "Stable and high-performance piezoelectric sensor via CVD grown WS_2," *Nanotechnology*, vol. 31, no. 44, Oct. 2020, Art. no. 445203, doi: 10.1088/1361-6528/aba659.

[17] Q. Liu, J. Chen, Y. Li, and G. Shi, "High-performance strain sensors with fish-scale-like graphene-sensing layers for full-range detection of human motions," *ACS Nano*, vol. 10, no. 8, pp. 7901–7906, Aug. 2016, doi: 10.1021/acsnano.6b03813.

[18] K. T. S. Kong, M. Mariatti, A. A. Rashid, and J. J. C. Busfield, "Enhanced conductivity behavior of polydimethylsiloxane (PDMS) hybrid composites containing exfoliated graphite nanoplatelets and carbon nanotubes," *Compos. B, Eng.*, vol. 58, pp. 457–462, Mar. 2014, doi: 10.1016/j.compositesb.2013.10.039.

[19] V. Jha, A. G. Thomas, M. Bennett, and J. J. C. Busfield, "Reversible electrical behavior with strain for a carbon black-filled rubber," *J. Appl. Polym. Sci.*, vol. 116, no. 1, pp. 541–546, 2010, doi: 10.1002/app.30556.

[20] K. Yamaguchi, J. J. C. Busfield, and A. G. Thomas, "Electrical and mechanical behavior of filled elastomers. I. The effect of strain," *J. Polym. Sci. B, Polym. Phys.*, vol. 41, no. 17, pp. 2079–2089, Sep. 2003, doi: 10.1002/polb.10571.

[21] J. Narongthong, S. Wießner, S. Hait, C. Sirisinha, and K. W. Stöckelhuber, "Strain-rate independent small-strain-sensor: Enhanced responsiveness of carbon black filled conductive rubber composites at slow deformation by using an ionic liquid," *Compos. Sci. Technol.*, vol. 188, Mar. 2020, Art. no. 107972, doi: 10.1016/j.compscitech.2019.107972.

[22] Z. Zhang et al., "Effect of carbon black on the strain sensing property of 3D printed conductive polymer composites," *Appl. Compos. Mater.*, vol. 29, no. 3, pp. 1235–1248, Jun. 2022, doi: 10.1007/s10443-022-10017-4.

[23] R. Nur, N. Matsuhisa, Z. Jiang, M. O. G. Nayeem, T. Yokota, and T. Someya, "A highly sensitive capacitive-type strain sensor using wrinkled ultrathin gold films," *Nano Lett.*, vol. 18, no. 9, pp. 5610–5617, Sep. 2018, doi: 10.1021/acs.nanolett.8b02088.

[24] J. Woo et al., "Ultrastretchable helical conductive fibers using percolated Ag nanoparticle networks encapsulated by elastic polymers with high durability in omnidirectional deformations for wearable electronics," *Adv. Funct. Mater.*, vol. 30, no. 29, Jul. 2020, Art. no. 1910026, doi: 10.1002/adfm.201910026.

[25] S. S. Banerjee et al., "Super-elastic ultrasoft natural rubber-based piezoresistive sensors for active sensing interface embedded on soft robotic actuator," *Appl. Mater. Today*, vol. 25, Dec. 2021, Art. no. 101219, doi: 10.1016/j.apmt.2021.101219.

[26] A. C. Yuen, A. A. Bakir, N. N. Z. M. Rajdi, C. L. Lam, S. M. Saleh, and D. H. B. Wicaksono, "Proprioceptive sensing system for therapy assessment using cotton fabric-based biomedical microelectromechanical system," *IEEE Sensors J.*, vol. 14, no. 8, pp. 2872–2880, Aug. 2014, doi: 10.1109/JSEN.2014.2319779.

[27] B. Park et al., "Nanoscale sensors: Dramatically enhanced mechanosensitivity and signal-to-noise ratio of nanoscale crack-based sensors: Effect of crack depth," *Adv. Mater.*, vol. 28, no. 37, p. 8068, Oct. 2016, doi: 10.1002/adma.201670259.

[28] S. Gong et al., "Tattoolike polyaniline microparticle-doped gold nanowire patches as highly durable wearable sensors," *ACS Appl. Mater. Interfaces*, vol. 7, no. 35, pp. 19700–19708, 2015, doi: 10.1021/acsami.5b05001.

[29] H. Zhang, W. Niu, and S. Zhang, "Extremely stretchable, stable, and durable strain sensors based on double-network organogels," *ACS Appl. Mater. Interfaces*, vol. 10, no. 38, pp. 32640–32648, Sep. 2018, doi: 10.1021/acsami.8b08873.

[30] Y. Wang et al., "Flexible electrically resistive-type strain sensors based on reduced graphene oxide-decorated electrospun polymer fibrous mats for human motion monitoring," *Carbon*, vol. 126, pp. 360–371, Jan. 2018, doi: 10.1016/j.carbon.2017.10.034.

[31] M. Cheng et al., "A review of flexible force sensors for human health monitoring," *J. Adv. Res.*, vol. 26, pp. 53–68, Nov. 2020, doi: 10.1016/j.jare.2020.07.001.

[32] X. Chen, D. Zhang, H. Luan, C. Yang, W. Yan, and W. Liu, "Flexible pressure sensors based on molybdenum disulfide/hydroxyethyl cellulose/polyurethane sponge for motion detection and speech recognition using machine learning," *ACS Appl. Mater. Interfaces*, vol. 15, no. 1, pp. 2043–2053, Jan. 2023, doi: 10.1021/acsami.2c16730.

[33] H. Zhang, D. Zhang, B. Zhang, D. Wang, and M. Tang, "Wearable pressure sensor array with layer-by-layer assembled MXene nanosheets/Ag nanoflowers for motion monitoring and human–machine interfaces," *ACS Appl. Mater. Interfaces*, vol. 14, no. 43, pp. 48907–48916, Nov. 2022, doi: 10.1021/acsami.2c14863.

[34] W. Zhao, D. Zhang, Y. Yang, C. Du, and B. Zhang, "A fast self-healing multifunctional polyvinyl alcohol nano-organic composite hydrogel as a building block for highly sensitive strain/pressure sensors," *J. Mater. Chem. A*, vol. 9, no. 38, pp. 22082–22094, Oct. 2021, doi: 10.1039/D1TA05586K.

[35] Y. Ma et al., "3D synergistical MXene/reduced graphene oxide aerogel for a piezoresistive sensor," *ACS Nano*, vol. 12, no. 4, pp. 3209–3216, Apr. 2018, doi: 10.1021/acsnano.7b06909.

[36] T. Yang, D. Xie, Z. Li, and H. Zhu, "Recent advances in wearable tactile sensors: Materials, sensing mechanisms, and device performance," *Mater. Sci. Eng. R, Rep.*, vol. 115, pp. 1–37, May 2017, doi: 10.1016/j.mser.2017.02.001.

[37] A. Georgopoulou, S. Michel, B. Vanderborght, and F. Clemens, "Piezoresistive sensor fiber composites based on silicone elastomers for the monitoring of the position of a robot arm," *Sens. Actuators A, Phys.*, vol. 318, Feb. 2021, Art. no. 112433, doi: 10.1016/j.sna.2020.112433.

[38] Y. He et al., "Wearable strain sensors based on a porous polydimethylsiloxane hybrid with carbon nanotubes and graphene," *ACS Appl. Mater. Interfaces*, vol. 13, no. 13, pp. 15572–15583, Apr. 2021, doi: 10.1021/acsami.0c22823.

[39] X. Xu et al., "Wearable CNT/$Ti_3C_2T_x$ MXene/PDMS composite strain sensor with enhanced stability for real-time human healthcare monitoring," *Nano Res.*, vol. 14, no. 8, pp. 2875–2883, Aug. 2021, doi: 10.1007/s12274-021-3536-3.

[40] M. Xu, J. Qi, F. Li, and Y. Zhang, "Highly stretchable strain sensors with reduced graphene oxide sensing liquids for wearable electronics," *Nanoscale*, vol. 10, no. 11, pp. 5264–5271, 2018, doi: 10.1039/C7NR09022F.

[41] Y. Jia et al., "Multifunctional stretchable strain sensor based on polydopamine/reduced graphene oxide/electrospun thermoplastic polyurethane fibrous mats for human motion detection and environment monitoring," *Compos. B, Eng.*, vol. 183, Feb. 2020, Art. no. 107696, doi: 10.1016/j.compositesb.2019.107696.

[42] E. Bilotti, R. Zhang, H. Deng, M. Baxendale, and T. Peijs, "Fabrication and property prediction of conductive and strain sensing TPU/CNT nanocomposite fibres," *J. Mater. Chem.*, vol. 20, no. 42, pp. 9449–9455, 2010, doi: 10.1039/C0JM01827A.

[43] T. Wu and B. Chen, "Autonomous self-healing multiwalled carbon nanotube nanocomposites with piezoresistive effect," *RSC Adv.*, vol. 7, no. 33, pp. 20422–20429, 2017, doi: 10.1039/C6RA28010B.

[44] Y. Nakaramontri, C. Kummerloewe, C. Nakason, S. Pichaiyut, S. Wisunthon, and F. Clemens, "Piezoresistive carbon-based composites for sensor applications: Effects of polarity and non-rubber components on shape recovery," *Exp. Polym. Lett.*, vol. 14, no. 10, pp. 970–986, 2020.

[45] J. G. Dabling, A. Filatov, and J. W. Wheeler, "Static and cyclic performance evaluation of sensors for human interface pressure measurement," in *Proc. Annu. Int. Conf. IEEE Eng. Med. Biol. Soc.*, Aug. 2012, pp. 162–165, doi: 10.1109/EMBC.2012.6345896.

[46] A. S. Sadun, J. Jalani, and J. A. Sukor, "Force sensing resistor (FSR): A brief overview and the low-cost sensor for active compliance control," *Proc. SPIE*, vol. 10011, Jul. 2016, Art. no. 1001112, doi: 10.1117/12.2242950.

[47] S. Kwon, S. Kim, I. Kim, Y. K. Hong, and S. Na, "Direct 3D printing of graphene nanoplatelet/silver nanoparticle-based nanocomposites for multiaxial piezoresistive sensor applications," *Adv. Mater. Technol.*, vol. 4, Dec. 2018, Art. no. 1800500, doi: 10.1002/admt.201800500.

[48] Y. Zheng et al., "Conductive thermoplastic polyurethane composites with tunable piezoresistivity by modulating the filler dimensionality for flexible strain sensors," *Compos. A, Appl. Sci. Manuf.*, vol. 101, pp. 41–49, Oct. 2017, doi: 10.1016/j.compositesa.2017.06.003.

[49] R. Zhang et al., "Strain sensing behaviour of elastomeric composite films containing carbon nanotubes under cyclic loading," *Compos. Sci. Technol.*, vol. 74, pp. 1–5, Jan. 2013, doi: 10.1016/j.compscitech.2012.09.016.

[50] C.-X. Liu and J.-W. Choi, "Analyzing resistance response of embedded PDMS and carbon nanotubes composite under tensile strain," *Microelectron. Eng.*, vol. 117, pp. 1–7, Apr. 2014, doi: 10.1016/j.mee.2013.11.013.

[51] J.-H. Kong, N.-S. Jang, S.-H. Kim, and J.-M. Kim, "Simple and rapid micropatterning of conductive carbon composites and its application to elastic strain sensors," *Carbon*, vol. 77, pp. 199–207, Oct. 2014, doi: 10.1016/j.carbon.2014.05.022.

[52] S. C. B. Mannsfeld et al., "Highly sensitive flexible pressure sensors with microstructured rubber dielectric layers," *Nature Mater.*, vol. 9, no. 10, pp. 859–864, Oct. 2010, doi: 10.1038/nmat2834.

[53] H. Deng et al., "Towards tunable resistivity–strain behavior through construction of oriented and selectively distributed conductive networks in conductive polymer composites," *J. Mater. Chem. A*, vol. 2, no. 26, pp. 10048–10058, 2014, doi: 10.1039/C4TA01073F.

[54] Y. R. Jeong, H. Park, S. W. Jin, S. Y. Hong, S.-S. Lee, and J. S. Ha, "Highly stretchable and sensitive strain sensors using fragmentized graphene foam," *Adv. Funct. Mater.*, vol. 25, no. 27, pp. 4228–4236, 2015, doi: 10.1002/adfm.201501000.

[55] A. Sanli, R. Ramalingame, and O. Kanoun, "Piezoresistive pressure sensor based on carbon nanotubes/epoxy composite under cyclic loading," in *Proc. IEEE Int. Instrum. Meas. Technol. Conf. (I2MTC)*, May 2018, pp. 1–5, doi: 10.1109/I2MTC.2018.8409527.

[56] M. Amjadi, K.-U. Kyung, I. Park, and M. Sitti, "Stretchable, skin-mountable, and wearable strain sensors and their potential applications: A review," *Adv. Funct. Mater.*, vol. 26, no. 11, pp. 1678–1698, Mar. 2016.

Sara Naderizadeh received the bachelor's degree in chemistry and the master's degree in polymer chemistry from the University of Tehran, Tehran, Iran, in 2010 and 2014, respectively, and the Ph.D. degree in the development of superhydrophobic polymer coatings from the Istituto Italiano di Tecnologia (IIT), Genoa, Italy.

She gains three years of experience in the industry. In September 2020, she took the role of a Research Fellow with the University of Surrey, Guildford, U.K., where her area of study involved investigating diffusiophoresis in polymer thin films. In November 2021, she joined the Queen Mary University of London (QMUL), London, U.K., as a Postdoctoral Research Assistant, contributing to the Business of Fashion, Textiles, and Technology (BFTT) Project. Her role within the project revolves around the development of more sustainable, circular, and intelligent wearables for the fashion and textile industry.

Giovanni Santagiuliana received the B.Sc. and M.Sc. degrees in materials science from the University of Padova, Padua, Italy, in 2009 and 2011, respectively, and the Ph.D. degree in graphene-based polymer nanocomposites from the Queen Mary University of London (QMUL), London, U.K., in 2018.

He has worked as a composite materials research and development specialist in the industry before obtaining his Ph.D. degree. In 2018, he became the Polymer Research Manager of Nanoforce Technology Ltd., Queen Mary University of London, a QMUL subsidiary focused on technology transfer to the industry. In November 2021, he started a part-time Postdoctor in the Business of Fashion, Textiles and Technology (BFTT) Project to develop more sustainable, circular, and intelligent wearables for the fashion and textile industry.

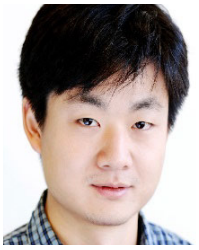

Wei Tu received the M.Eng. degree in materials and business and the Ph.D. degree in materials from the Queen Mary University of London, London, U.K., in 2004 and 2011, respectively.

He has been working as the Materials Scientist of Nanoforce Technology Ltd., since 2008, facilitating commercial collaborative research and development projects and consultancy projects. In 2019, he joined Nurvv Ltd. (formerly Impact Tech Labs), London, as the Materials Scientist and later become the Sensor Product Manager for Smart Wearable Consumer Products. In 2021, he became the Project Lead of a Sustainable Sensor Project with the Business of Fashion, Textiles and Technology (BFTT) to develop novel flexible force sensors for wearables. His research interests include high-performance polymers and fibers, conductive polymeric composites, nanomaterials, natural fiber composites, and dielectric polymer materials.

Derek Marsh, photograph and biography not available at the time of publication.

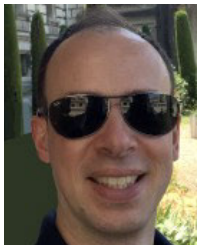

Emiliano Bilotti received the Laurea degree (equivalent to M.Eng.) in materials engineering from the University of Naples "Federico II," Naples, Italy, in 2004, and the Ph.D. degree from the Materials Department, Queen Mary University of London, London, U.K., in 2009.

He is currently a Senior Lecturer (equivalent to an Associate Professor) in Multifunctional Polymer Composites with the Department of Aeronautics, Imperial College London, London. His research interests include polymer composites for energy storage (capacitors), energy harvesting (organic thermoelectric, ferroelectric, and piezoelectric), smart polymer composites (sensors, pyro-resistivity for self-regulating heater, and actuation/shape programming) and biopolymers (collagen and silk).

James J. C. Busfield received the M.A. degree in engineering science from the University of Oxford, Oxford, U.K., in 1989, and the Ph.D. degree in materials science from the Queen Mary University of London, London, in 2000.

He has been the Head of the Soft Matter Group, Queen Mary University of London, for more than a quarter of a century. His research group is currently the largest research group working on soft matter in U.K. His team examines the physical behavior by experiment and modeling techniques of elastomers and rubber materials. His properties of interest include abrasion, friction, fracture, creep, fatigue, viscoelastic behavior, modulus enhancement, self-healing, recycling, aging, and composite filler reinforcement. His group also develops smart soft materials that can sense their environment or that can change shape in response to a physical stimulus.

Dr. Busfield was a National Teaching Fellow in 2009 and a Fellow of the Royal Academy of Engineering in 2020. He has been recognized for his research by the award of the Colwyn Medal (by IOM3) in 2009, the Sparks-Thomas Award (by ACS) in 2010, and the George Stafford Whitby Award (by ACS) in 2021.